Coupling of capillary RBC flow failure with neuronal depolarization

Minoru Tomita[1], Yutaka Tomita[1,2], Haruki Toriumi[1], Miyuki Unekawa[1] & Norihiro Suzuki[1]

1. Department of Neurology, School of Medicine, Keio University, Tokyo Japan
2. Department of Preventive Medicine for Cerebrovascular Disease, School of Medicine, Keio University, Tokyo Japan

Running title: Neuro-capillary coupling during CSD

Date of submission:	May 4, 2009
Main text:	2384 words
Abstract:	147 words
Figures:	7 items (4 color figures)
Number of references:	26
Supplementary Figures	
1. Motion pictures 1:	878 KB
2. Motion picture 2:	273 KB

Correspondence to: Minoru Tomita[1] e-mail: mtomita@sc.itc.keio.ac.jp

Abstract

RBC (oxygen-carrier) behaviour in the cerebrocortical microvasculature during K^+-induced cortical spreading depression (CSD) was examined in urethane-anesthetized male Wistar rats (n=10). The movements of FITC-labeled RBCs in single capillaries in the cortical region were traced with a high-speed camera laser scanning confocal fluorescence microscope and analyzed with Matlab domain software, KEIO-IS2, to obtain the velocities of all labeled RBCs appearing in local capillaries during CSD wave propagation. We found that CSD induced periodic decreases in both RBC number and velocity until RBCs halted or disappeared for 3.3 ± 2.3 s, and then RBC flow was restored. The RBC flow stall was statistically significant ($P < 0.05$). During capillary flow failure in association with CSD spread, systemic arterial blood pressure remained unchanged. We conclude that RBCs are transiently sieved and stalled in capillaries during neuronal depolarization, and we suggest that this neuro-capillary coupling involves a hemorheological (viscosity-related) mechanism.

Introduction

Cortical spreading depression (CSD), originally reported by Leão[1] as a spreading zone of EEG flattening following topical application of toxin to rabbit cerebral cortex, is now thought to be a fundamental process commonly involved in acute brain disorders[2]. The nature of CSD, however, remains largely unknown. Microvascular changes concomitant with CSD may be involved in clinical events, such as migraine, brain injury and stroke, and the phenomenon has thus drawn the attention of not only basic scientists, but also clinicians. In a previous study[3], using a hemodilution technique applied to a small area with high resolution (pixels of 40x40 μm^2)[4] in α-chloralose-urethane-anesthetized rats, we found that K^+-induced CSD caused cessation of local capillary flow for a few seconds, in association with the wave-ring spread of optical transmission changes of the rat cerebral cortex. The physiological relevance of the cessation of capillary flow in the region of interest (ROI) might seem questionable, however, on the grounds that capillary flow has to be continuous to supply oxygen to neurons, unless the neurons have died. In fact, it has often been observed that, even if the perfusion pressure suddenly falls to zero (e.g., following cerebral arterial occlusion, or electrically induced cardiac arrest) brain capillary flow does not totally stop immediately, because it is protected presumably by residual vasomotor action of the cerebral vessels. Therefore, one might consider that transient cessation of local capillary flow in the brain under conditions of normal blood pressure and sustained normal local perfusion pressure, as in the case of CSD, would not be likely. The apparent capillary flow stop could have been due to misinterpretation of the data obtained by observation of the disappearance of hemodilution curves, which was reported by us previously[3].

In this paper, we aimed to examine RBC behaviour per se directly in capillaries in the ROI, in order to obtain unequivocal evidence of rapid and transient RBC flow in the group of capillaries halt during CSD, using a new method of high speed camera laser scanning confocal fluorescence microscopy developed by us[5].

Results

General Observation

We confirmed that CSD was induced by topical application of K^+ in all 8 rats, appearing as negative deflections of approximately 9.4 ± 3.8 mV (ranging -5 and -13 mV) and 1.2 ± 0.3 min duration in DC recordings; these deflections occurred 5 or 6 times successively at intervals of a few minutes. The speed of spreading CSD waves was approximately 3.8 ± 0.9

mm/min. We also confirmed that saline did not induce CSD in 2 cases. The mean systemic arterial blood pressure (SABP) recorded was 98.2 ± 4.6 mmHg before CSD. It remained unchanged during CSD, and was 97.5 ± 3.2 mmHg after the final episode of CSD. The difference of SABP before and after CSD was not statistically significant.

RBC behaviour in capillaries in controls

When FITC-labeled RBCs were injected into the circulating blood, labeled RBCs appeared in the cortical microvasculature, including capillaries, arterioles and veins, as bright particles like fireflies over a dark background. RBCs running along capillaries were focused with a water immersion lens of 60x attached to an intravital fluorescence microscope. The RBC flow in capillaries appeared to be continuous and stationary to the naked eye. When it was recorded on a video camera at 30 fps, the RBC flow in a single capillary was by no means stationary and continuous. As will be described quantitatively later, RBC flow was highly heterogeneous: the manner of flow and the separation of successive RBCs were variable in space and time (Fig. 1). Some RBCs sliding near the arteriolar wall would slip into a capillary and remained close to the endothelial wall of the capillary, while others moved in the central part of the internal lumen. RBC flow was not smooth along the capillary: it slowed at certain locations while it ran quickly at other locations, even though there was no apparent morphological change in the capillary lumen. At some capillary inlets, RBCs appeared to jump as if they were powered by a spring or to be sucked up by the capillary, and their speed became 2 or 3 times faster than that when they were moving through the feeding arteriole (Supplementary Figure 1). We were not able to detect any diametric changes at the so-called ‘precapillary sphincter’ when RBCs moved through at varying speeds. At branching site of capillaries where a capillary was divided into left and right branches, RBC distribution was just unpredictable. In some cases, 4 or 5 RBCs went to the left successively, while at the next moment more RBCs moved to the right. Again, we were not able to see any diametric change (vasomotion) of the branching capillaries at the occasion of ‘switching’. On one occasion, 2 RBCs adhering to each other came to a branching site, stayed at the center for a moment, then suddenly separated, and one went to right and the other to the left simultaneously (Supplementary Figure 2). A typical example of computer analysis of a videoclip (1.2 s) is shown in Figure 2. Figure 2a, 2b, and 2c are serially arranged velocity maps of RBCs obtained separately from subsections (0.4 s each) of the videoclip. RBCs that appeared in the capillaries in the

ROI during each 0.4 s were numbered in the order of appearance and automatically traced frame-by-frame, to calculate velocity changes. The different colors denote levels of RBC velocity scaled on the right, and the mosaic shows heterogeneity of RBC flow along the capillaries. Note that color distributions were different even in corresponding capillaries, indicating a temporal heterogeneity on the time scale of 0.4 s. The velocity maps evidenced that RBC movements in capillaries were by no means stationary and constant, but responded dynamically on a short time scale, presumably to neuronal requirements. The velocities seldom fell to zero; RBCs maintained speeds in the range of approximately 0.5-3.0 mm/s with specific cyclic fluctuations in the range of approximately 0.5-0.1 cycles per s in this case. In short, under physiological conditions RBCs kept moving without stagnation, but heterogeneously, through the highly tortuous intraparenchymal capillaries. When treated as whole capillaries, the average velocity of RBCs at 250 Hz in 8 rats was 1.46 ± 1.13 mm/s, with a range of 0.77 to 3.58 mm/s, and the cyclic fluctuation was ca. 0.36 ± 0.17 cps (or ca. 21.6 cycles per min) in the control state. Figure 3 shows a typical example of a velocity profile of 220 RBCs that appeared during 4 s (2000 frames) in vessels in the ROI of 400 μm x 600 μm; the vessels were confirmed to be capillaries by the technique reported previously[6]. Note that velocities of capillary RBCs averaged around 1.7 mm/s, but some reached as high as 7.5 mm/s in this case.

RBC behaviour in capillaries during CSD

When CSD was propagating, the background brightness of the cortical area decreased as reported previously[3,7]. As the darkening progressed, RBCs in capillaries showed a gradual reduction in velocity (Fig. 4a) and number (Fig. 4b), and finally stopped/disappeared. Figure 5a, 5b, and 5c show an enlarged single capillary at the peak of CSD passage. RBCs had become round owing to reduced shear stress and the plasma appeared to be optically heterogeneous, which may indicate that the plasma was sludgy and viscous. Figure 5a shows an RBC slowly moving in the viscous capillary. The capillary became empty with no labeled RBCs for a moment (Fig. 5b). An RBC apparently adhered to the capillary wall and stayed there without movement (Figure 5c). After 10 – 20 s the background became brighter, preceding the flow recovery, and then RBCs resumed movement until complete recovery to the previous state was attained. It should be noted that the diameter of the capillary did not narrow at the time of RBC stoppage, but rather even became wider when compared with that in the control state. Plasma flow, and therefore RBC flow, became

sluggish, presumably in response to viscosity change of the plasma. Figure 6 exhibits the chronological arrangement of 48 sequential RBC velocity maps (0.4 s each at 250 Hz or 100 frames each). The velocity maps show that RBC movements decreased gradually and finally disappeared, as can be seen in the red-flagged pictures; the flag indicates no detectable RBC movement or no RBC appearance in capillaries in the ROI. The period of no RBC movement in the ROI was approximately 8 s in this case. In the frames at 15.6 and 16.8 s, minimal movements of one or two RBCs could be seen within the flagged sequence. We ignored these "ghost" movements in estimating the period of no RBC movement, because they would have no physiological significance for oxygen transport. Fig. 7 shows a summary of all eight arrays of compressed velocity profiles aligned on the 12 s interval each. The arrows indicate the flagged period of RBC flow stoppage/disappearance. The occurrence of the no-RBC period in all 8 cases was statistically significant ($p < 0.05$, unpaired t test for the null hypothesis). The average period of RBC disappearance was 3.3 ± 2.3 s (0.8 s to 6.8 s). Resumption of RBC movements was gradual, though this is not shown in Figure 7.

Discussion

The RBC flow heterogeneity along capillaries in the control state can not be explained by traditional arterial regulation of blood flow with passive compliant capillary flow changes. Kleinfeld et al.[8], employing two-photon imaging, described individual capillary flow in layer 4 of the rat cerebral cortex as follows: 'it was highly irregular flow in which the speed and flux changed suddenly or in which individual RBCs stalled for a certain period of time'. Our observation in layer 1 was quite similar to this. RBC flow velocity and number were fluctuating in the control state, presumably responding to the time-to-time requirements of neurons. They observed RBC stall in a single capillary, but we found that RBCs stalled/disappeared from all capillaries in the ROI when a group of neurons were depolarized during CSD. In this period, plasma was present, either flowing or not flowing, in the capillaries when RBCs were absent. The condition was not due to capillary closure at the capillary sphincter, or 'capillary de-recruitment'. No capillary recruitment in the brain microvasculature in the sense of opening of the precapillary sphincter was observed by Gobel et al.[9] during hypercapnia or by Pinard et al.[10] during reactive hyperemia. The periodic changes in RBC number and velocity in capillaries resulted from perfusion and nonperfusion of RBCs through capillaries, as described by Hudetz[11]. Our data also revealed

apparent ‘active’ capillary density changes, as seen by occasional geometric changes in the number of RBC-present capillaries, which is in agreement with the concept of apparent capillary density by physiological recruitment[12]. Local capillary RBC flow may be regulated by neurons through the enigmatic RBC ‘sieving effect’, since we observed that capillary RBC flow failure became conspicuous in the ROI when CSD passage or local neuronal depolarization was induced. Akgoren and Lauritzen[13] observed that functional recruitment of RBCs to the rat cerebellar cortex accompanied increased neuronal activity when cerebellar neurons were activated by electrical stimulation of parallel and climbing fibers. Our results may show a reverse aspect of neuro-capillary coupling, i.e., transient neuronal dysfunction associated with geometric RBC de-recruitment and local capillary flow cessation. However, there were no detectable diametric changes of capillaries in association with the RBC flow failure, but only a sludgy appearance during CSD, which may suggest the operation of some hemorheological flow resistance control.

Our working hypothesis on the capillary flow failure at present is as follows. After passing through the resistance vessels, RBCs seem to enter an isolated extraterritorial area of circulation where no arterial governance extends. RBCs here are in the extremely low Reynolds number world where vessel diametric changes are meaningless. RBCs can run freely throughout the plasma canal along with the multiplex plasma streams in the capillary network. Spatial distribution of RBCs is determined, thereafter, not by vessel diametric changes, against Krogh’s capillary sphincter model, but presumably by variability in flow resistance or subtle viscosity changes in capillary channels. The capillary network is not “single inlet and single outlet”, but “multiple inlets and multiple outlets”. RBCs have no obligatory channel to pass through. If the flow resistance of a certain group of capillary channels increases, even only slightly, RBCs tend to detour around these channels and RBC exclusion may occur. The rapid increase in local capillary flow resistance might be induced by the mass effect of “explosive” astroglial cell swelling upon CSD passage[3]. The occurrence of such rapid astroglial cell swelling during CSD is supported by the observation of rapid Na^+ and Cl^- movement into astroglial apical dendrites[14,15], a rapid cerebral impedance drop[16], changes in extracellular diffusion parameters as judged by morphological analysis with a confocal microscope[17] and a transient apparent diffusion coefficient decrease (fluid shift from extracellular space into cellular components) detected by magnetic resonance imaging[18]. However, as mentioned previously we were not able to observe any diametric changes in capillaries during CSD. We consider that the extracellular

fluid shift would cause a decrease in the extracellular space and swelling of astroglia, but the swelling of cells would occupy only the extracellular space, not the vascular space. Our data show that capillary flow resistance could be a consequence of very small (practically undetectable) narrowing of the capillary internal lumen by the thickening of the glycocalyx (buffy coat) on the endothelial cells[19,20,21] or resultant viscosity changes which would increase capillary flow resistance. Fibrinogen may participate in the viscosity change. The effect of astroglial cell swelling upon CSD passage as described above might not result in direct compression of capillaries, but rather separation of opposing basement membranes of astroglia and endothelial cells, thereby disconnecting intimate signaling transactions between astroglia and endothelial cells. It seems likely that endothelial cells per se also became depolarized during CSD passage (Fig. 5).

We cannot deny the participation of feeding arterioles of 15-30 μm in diameter during CSD, since our previous observations[22] revealed strong vasoconstriction followed by marked sustained vasodilatation of arterioles of about 25 μm in diameter during K^+-induced CSD in cat cerebral cortex. Participation of interneurons in such local flow regulation is also possible[23]. It could be not direct, but rather may contribute to coordinated or compensatory changes, since such a biphasic diametric change is incompatible with the capillary RBC flow changes reported here.

Material and methods

Ten Wistar rats were used. Experiments were approved by the Animal Ethics Committee of Keio University. Each rat under intraperitoneal urethane anesthesia following halothane was fixed to a head-holder, and a window was opened in the skull at the temporo-parietal region of the cerebral cortex. A femoral artery and a femoral vein were catheterized for blood pressure monitoring and injection of tracers. The dura was removed, and the cortex was exposed. The head-holder with the rat was placed so that the brain was beneath a intravital microscope (switchable between a conventional (30 fps) videocamera and high-speed (250-500 fps) camera, both installed in the laser scanning confocal fluorescence microscope) which was developed by us and reported previously[5]. Briefly, the assembly comprises an objective lens (LU Plan EPI SLWD 65 20x N.A.=0.35, and 50x N.A.=0.55), an argon laser (λ=488, Melles Griot, Carlsbad, CA, USA), a multibeam confocal scanning 70 unit (CSU22; Yokokawa, Tokyo, Japan), an image intensifier (C6653MOD-N; Hamamatsu Photonics, Hamamatsu, Japan), a stage with x-y-z knobs, a MotionPro

high-speed camera (125-500 frames/s or 125-500 Hz; shutter speed of 1/125-1/1000 s) with a digital imaging system (RED-Lake, San Diego, CA., USA) and a high vision camera (HDR-HC3, HDV 1080, Sony, Tokyo, Japan) for on-line video-recording (30 Hz). A halogen lamp was used for a general illumination of brain microcirculation and astroglia with the video camera. The important point here is the wide working distance (the distance from the objective lens to the brain surface when the water immersion lens was not in use) of 1.5 cm, which is convenient for concomitant measurement of field potential, staining astroglia and topical application of K^+ solution to induce CSD (n=8). When needed we used the water immersion lens (Plan Fluor 60x W N.A.=1.00; Nikon, Tokyo, Japan). After selecting an appropriate capillary-rich ROI of about 450 μm x 600 μm in use of 20 x lens or 75 μm x 100 μm in use of 60 x lens in the cerebral cortex 50-80 μm below the pia, 0.5 ml of fluorescein isothiocyanate (FITC)-labeled RBC suspension, prepared beforehand according to Seylaz et al.[24], was injected into the blood stream through the venous catheter. We found that the final concentration in the circulating blood was approximately 0.4 % of whole-body blood RBC. In all experiments, SABP was routinely monitored. FITC-labeled RBCs injected into the femoral vein were seen flowing through arterioles, capillaries, and veins of the cerebral cortical microvasculature on the monitor screen through the high vision camera. In 4 rats, fluorescent sulforhodamine-101[25] was directly applied on the exposed brain surface to stain astroglia. The dye was washed away with saline after 3 min. CSD was induced by topical injection of a very small amount of K^+ solution (150 mM) into the cortex approximately 5 mm posterior to the ROI. The same amount of saline was applied in 2 control rats. An Ag-AgCl electrode 100 μm in diameter was placed between the ROI and the K^+ injection site (approximately 2 mm posterior to the center of the ROI) for DC field potential recording with reference to another Ag-AgCl electrode inserted into the soft tissue between the skull and scalp. The DC potential and SABP were recorded on a personal computer with Acqknowledge software (MP 100 WS). The video clip from the high-speed camera was transferred to the PC and analyzed with Matlab domain software (KEIO-IS2), which was developed in our laboratory[26]. The program exploits the light intensity difference between the dark background and the light, round particles in the visual field of the microscope to track the particles automatically. The algorithm for RBC tracking, velocity and total number was described elsewhere[5]. The principle was that the computer recognized all FITC-labeled RBCs' locations (the centroids of the RBC image) frame by frame, measured the displacement distances of individual RBCs during the interval between

frames, and calculated the velocities by multiplying the result by the frame rate. For each high-speed frame set, the computer automatically generated four maps: an RBC tracking map, an RBC velocity map, an RBC number (density) map, and an RBC velocity profile. If there was no RBC movement in a given set of frames, the computer flagged this set of frames. However, the computer just detected movements of recognized particles, but could not discriminate RBC disappearance from RBC halt. In other words, the flag includes uncounted RBCs flowing slower than the lower limit of measurable velocity, and does not necessarily mean 'no RBC' in vessels. However, these conditions are the same in the sense that oxygen delivery is impaired in both cases. In calculating RBC velocities, the software made no correction for movement along the z-axis, but simply expressed the results as a two-dimensional (x-y) RBC velocity map. The velocity data were then exported to a spreadsheet (Microsoft Excel), where the average velocities of all individual RBCs that appeared in the ROI during a selected period were listed. After the velocities were sorted in order of magnitude, the data were presented as a bar graph. This graph illustrates the velocity profile of RBCs that appeared in the ROI during a specified period, containing all the information needed for the present investigation: the bar height represents RBC velocity, and the abscissa shows the number of RBCs. The number of RBCs was broadly considered to represent either relative capillary density or local tissue hematocrit at that moment. Since the computer RAM memory was limited, camera recording was limited to only 6000 frames or 24 s at 250 Hz and only 12 s at 500 Hz. Therefore, during CSD, acquisition of data started at the peak of CSD. The recorded data set was divided into five or six data subsets and analyzed for RBC velocity changes as described above. If there was no RBC movement in a given set of frames, namely, no RBC movement in all microvasculature including capillaries in the ROI the computer flagged this set of frames. If no sequence was flagged, we repeated the calculation for a reduced set of 100 frames. The analyzed data were displayed in sequential arrangement of compressed velocity profiles.

Note: Supplementary information is available on the Nature Neuroscience website.

Acknowledgements

This work was supported by JSPS Grant-in-Aid #17390255. The authors have no conflicts of interest. We thank Otsuka Pharmaceutical Co., Ltd. and Pfizer Japan Inc. for their financial support. There is no conflict of interest.

Author Contributions

Minoru Tomita and Norihiro Suzuki designed the experiments, Yutaka Tomita, Haruki Toriumi and Miyuki Unekawa conducted the experiments and collected the data, and Minoru Tomita wrote the manuscript with the help of all the other authors.

References

1. Leão, A.A.P. Spreading depression of activity in cerebral cortex. *J. Neurophysiol.* **7**, 359-390 (1944).
2. Hansen, A.J. & Lauritzen, M. The role of spreading depression in acute brain disorders. *An. Acad. Bras. Cienc.* **56**, 457-479 (1984).
3. Tomita, M. et al. Initial oligemia with capillary flow stop followed by hyperemia during K^+-induced cortical spreading depression in rats. *J. Cereb. Blood Flow Metab.* **25**, 742-747 (2005).
4. Schiszler, I., Tomita, M., Fukuuchi, Y., Tanahashi, N. & Inoue, K. New optical method for analyzing cortical blood flow heterogeneity in small animals: validation of the method. *Am. J. Physiol*. **279**, H1291-H1298 (2000).
5. Tomita, M. et al. Automated method for tracking vast numbers of FITC-labeled RBCs in microvessels of rat brain in vivo using a high-speed confocal microscope system. Microcirculation **15**, 163-174 (2008).
6. Unekawa, M. et al. Frequency distribution function of RBC velocities in single capillaries of the rat cerebral cortex using intravital confocal microscope with high-speed camera. *Asian Biomed*. **2**, 203-218 (2008).
7. Tomita Y. et al. Repetitive concentric wave-ring spread of oligemia/hyperemia in the sensorimotor cortex accompanying K^+-induced spreading depression in rats and cats. *Neurosci Lett* **322**,157-60 (2002).
8. Kleinfeld, D., Mitra, P.P., Helmchen, F. & Denk W. Fluctuations and stimulus-induced changes in blood flow observed in individual capillaries in layers 2 through 4 of rat neocortex. *Proc. Natl. Acad. Sci. USA* **95**, 15741-15746 (1998).
9. Gobel, U., Theilen, H., Schrock, H. & Kuschinsky, W. Dynamics of capillary perfusion in the brain. *Blood Vessels* **28**, 190-196 (1991).
10. Pinard, E., Engrand, N. & Seylaz, J. Dynamic cerebral microcirculatory changes in transient forebrain ischemia in rats: involvement of type I nitric oxide synthase. *J Cereb Blood Flow Metab* **20**,1648-1658 (2000).
11. Hudetz, A.G. Blood flow in the cerebral capillary network: a review emphasizing observations with intravital microscopy. *Microcirculation* **4**, 233-52 (1997).
12. Gjedde, A., Poulsen, P.H. & Ostergaard, L. On the oxygenation of hemoglobin in the human brain. *Adv. Exp. Med. Biol.* **471**:67-81 (1999).

13. Akgoren, N. & Lauritzen, M. Functional recruitment of red blood cells to rat brain microcirculation accompanying increased neuronal activity in cerebellar cortex. *Neuroreport* **10,** 3257-3263 (1999).
14. Van Harreveld, A. & Schade, J.P. Chloride movements in cerebral cortex after circulatory arrest and during spreading depression. *J. Cellular comp. Physiol*. **54**, 65-77 (1959).
15. Tomita, M. Increased intracranial pressure and brain edema. In: *Pathology & Genetics. Structure and functions of CNS blood vessels, Cerebrovascular Diseases* (Kalimo, H. ed.), Chapter 5, ISN Book Series, Neuropath Press, Basel, Switzerland, pp.39-49 (2005).
16. Van Harreveld, A. & Ochs, S. Cerebral impedance changes after circulatory arrest. *Am.. J. Physiol.* **187**, 180-192 (1956).
17. Anderová, M. et al Effect of elevated K^+, hypotonic stress, and cortical spreading depression on astrocyte swelling in GFAP-deficient mice. *Glia* **35**, 189-203 (2001).
18. De Crespigny, A., Rother, J., van Bruggen, N., Beaulieu, C. & Moseley, M.E. Magnetic resonance imaging assessment of cerebral hemodynamics during spreading depression in rats. *J. Cereb. Blood Flow Metab.* **18**, 1008-1017 (1998).
19. Vogel, J. et al. Influence of the endothelial glycocalyx on cerebral blood flow in mice. *J. Cereb. Blood Flow Metab.* **20**, 1571-1578 (2000).
20. Pries, A.R., Secomb, T.W. & Gaehtgens, P. The endothelial surface layer. *Pflugers Arch.* 440, 653-666 (2000).
21. Pries, A.R. et al. Microvascular blood flow resistance: role of endothelial surface layer. *Am. J. Physiol.* **273**, H2272- H2279 (1997).
22. Osada, T., Tomita, M., Suzuki, N.. Spindle-shaped constriction and propagated dilation of arterioles during cortical spreading depression. *Neuroreport* **17**, 1365-1368 (2006).
23. Cauli, B. et al. Cortical GABA interneurons in neurovascular coupling: relays for subcortical vasoactive pathways. *J. Neurosci.* **24**, 8940-8949 (2004).
24. Seylaz, J. et al. Dynamic in vivo measurement of erythrocyte velocity and flow in capillaries and of microvessel diameter in the rat brain by confocal laser microscopy. *J. Cereb. Blood Flow Metab.* 19: 863-870 (1999).
25. Nimmerjahn, A., Kirchhoff ,F., Kerr, J.N. & Helmchen, F. Sulforhodamine 101 as a specific marker of astroglia in the neocortex in vivo. *Nat Methods* **1**, 31-37 (2004).

26. Schiszler. I. et al. Software (KEIO-IS2) for automatically tracking red blood cells (RBCs) with calculation of individual RBC velocities in single capillaries of rat brain (abstr.). *J. Cereb. Blood Flow & Metab.* **25,** S541 (2005).

Acknowledgment

This work was supported by JSPS Grant-in-Aid # 17390255.

Figure legends

Figure 1: FITC-labeled RBCs and control capillary.
Three RBCs are moving through a capillary (a) and 2 RBCs move through the same capillary 0.4 s later (b). The capillary wall was unintentionally stained with FITC dextran that leaked from FITC-stained RBCs. Note there are bright orange spots attached to the capillary wall which could be astroglia stained with sulforhodamine 101. Astroglial elements appear to protrude into the capillary lumen. (60x water immersion lens, $\lambda = 488$ laser beam).

Figure 2: Three sequential RBC velocity maps.
The maps were automatically computed from a video clip: 0.4 s at 250 Hz, 100 frames. Note mosaic color changes showing heterogeneity of RBC velocity changes in capillaries varying in space and time. All RBCs detected by the computer were numbered automatically in the order of appearance, separately in each map. The total number may be broadly related to dynamic changes in tissue hematocrit, RBC recruitment, and capillary density change during the limited period of videoclip acquisition.

Figure 3: A velocity profile.
A typical example of velocity profile of RBCs in capillaries in the ROI is shown. Two hundred and nine RBC velocities were collected from capillaries in the ROI during the period of 2 s at 500 Hz (1000 frames). The velocity ranges from 0.4 mm/s to 7.0 mm/s.

Figure 4: Capillary RBCs and CSD.
Variation in average RBC velocity and number in the ROI is shown. RBC velocities and number appearing in capillaries in the ROI were obtained every 0.4 s at 250 Hz from videoclip recorded during CSD. The average velocity and total RBC number were calculated, and plotted against time in s. Though fluctuating, these parameters reached zero, and this value persisted for 8 s.

Figure 5: Capillary images during CSD.
The images of a capillary were obtained from a videoclip recorded during the peak of propagating CSD. When compared with those of normal capillaries (Fig. 1) the capillary

images look rather blurred, due probably to membrane depolarization of endothelial cells per se. (When viewing cultured human brain endothelial cells with a video-enhanced-contrast differential-interference-contrast microscope we noticed that vivid cells looked sharp in contour, while depolarized cells looked blurred). Slowly flowing RBC appears round (Fig. 5a), without high-shear-induced deformation. One RBC was stuck to the wall (Fig. 5c).

Figure 6: A panoramic presentation of sequential RBC velocity maps during CSD.
Images were produced sequentially from a video clip; 24 s at 250 Hz, 6000 frames recorded during CSD passage. Note the appearance of flagged (red) sequences (no movement of RBCs) for ca. 8.8 s from 8.8 s to 17.2 s. After the frame of 17.2 s, RBCs restarted to appear again, and the previous flow status was restored.

Figure 7: Groups of arrayed velocity profiles.
Flags (RBC stops) appeared in all 8 cases as indicated by arrows.

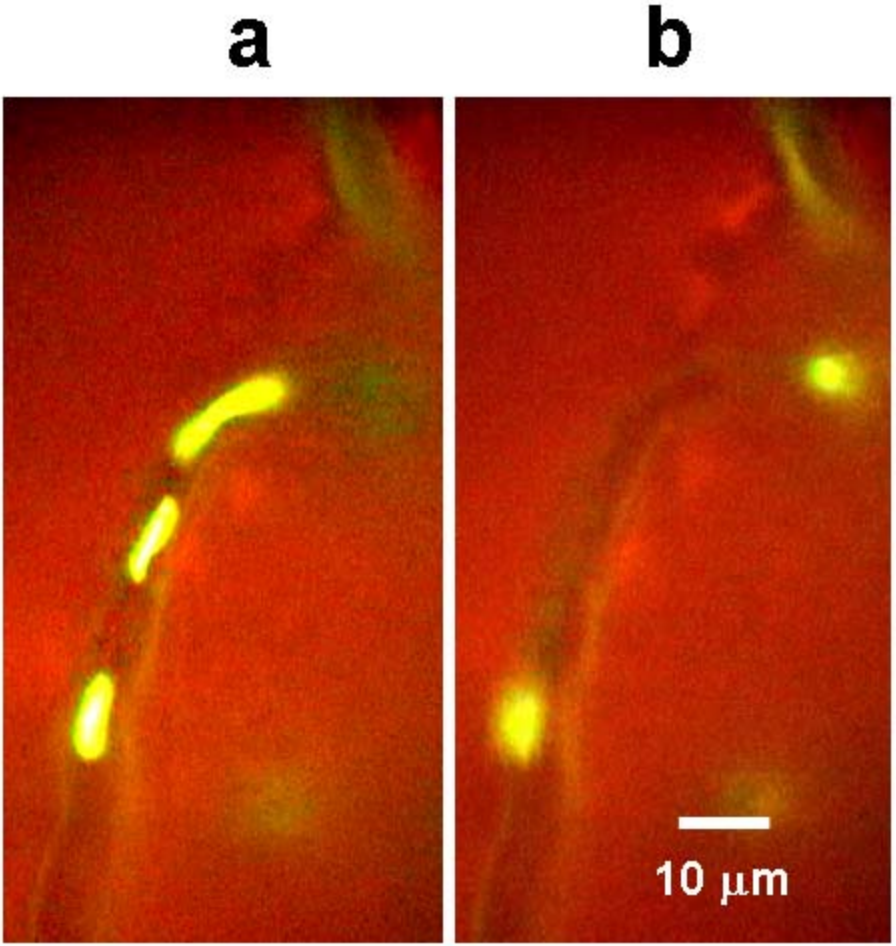
a
b
10 μm

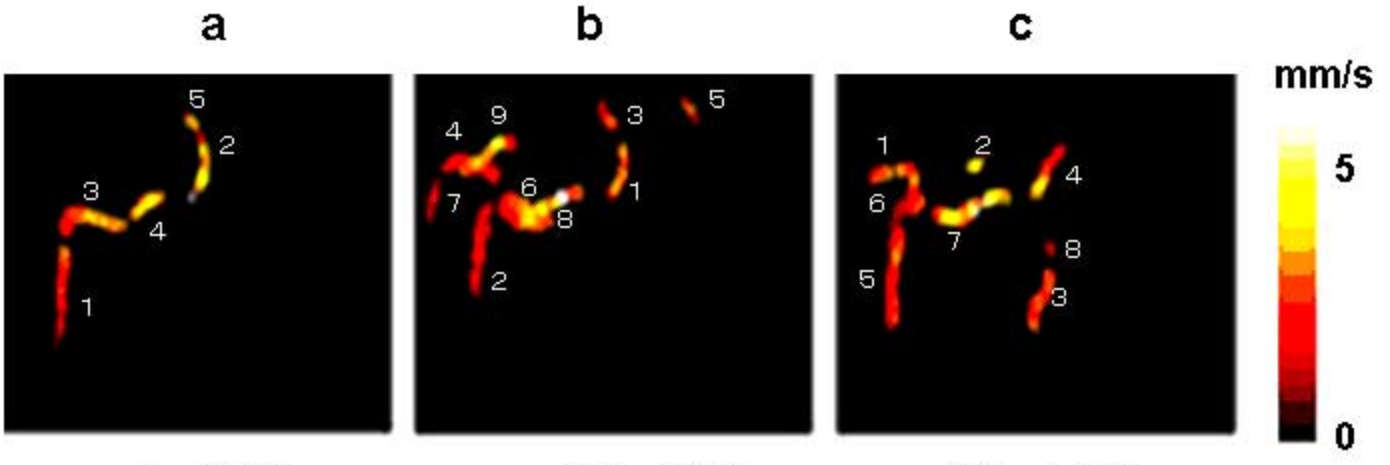
a
b
c
mm/s
5
0
0 – 0.4 s
0.4 – 0.8 s
0.8 – 1.2 s

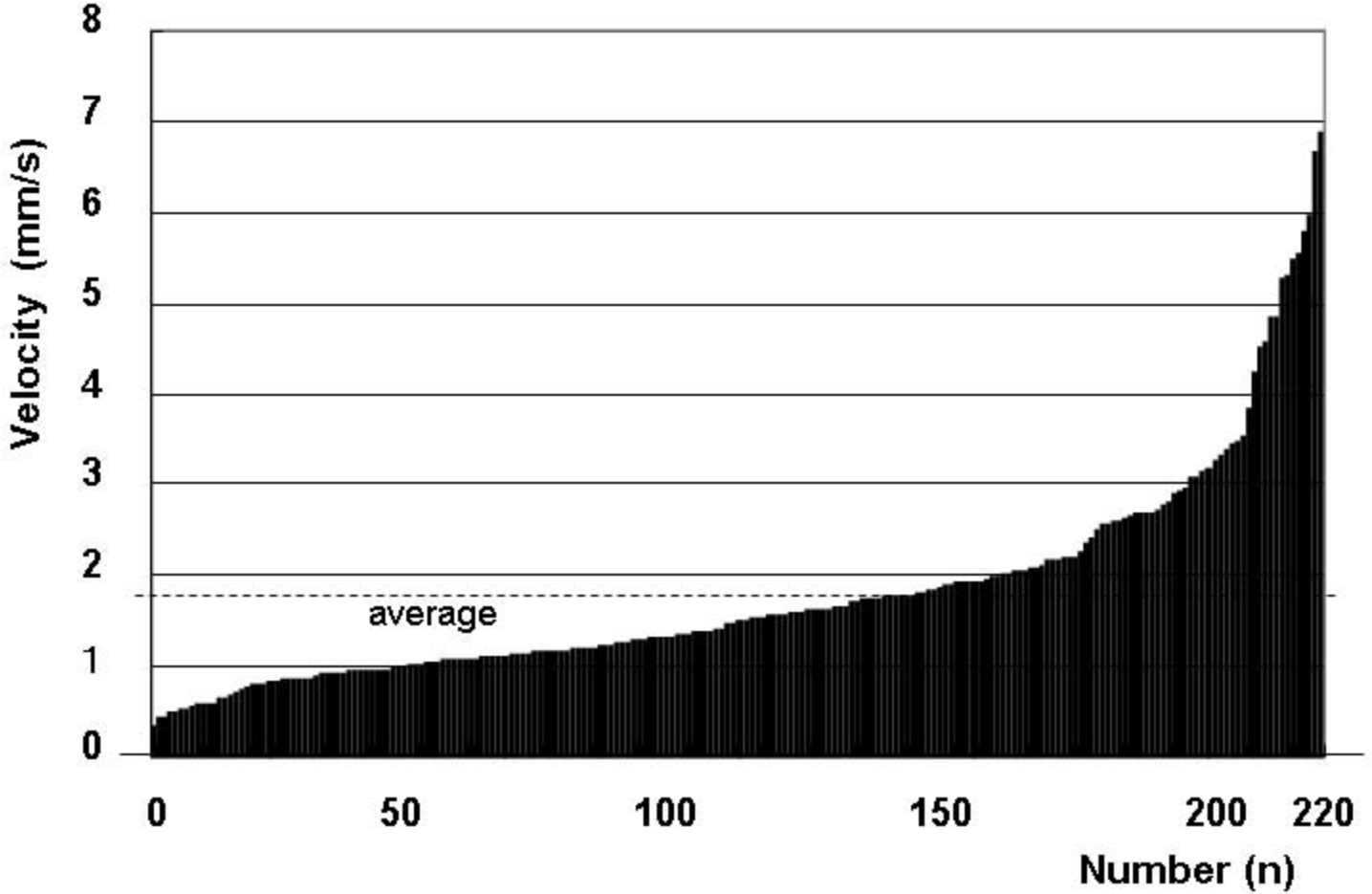
8
7
6
5
4
3
2
1
0
Velocity (mm/s)
average
0
50
100
150
200
220
Number (n)

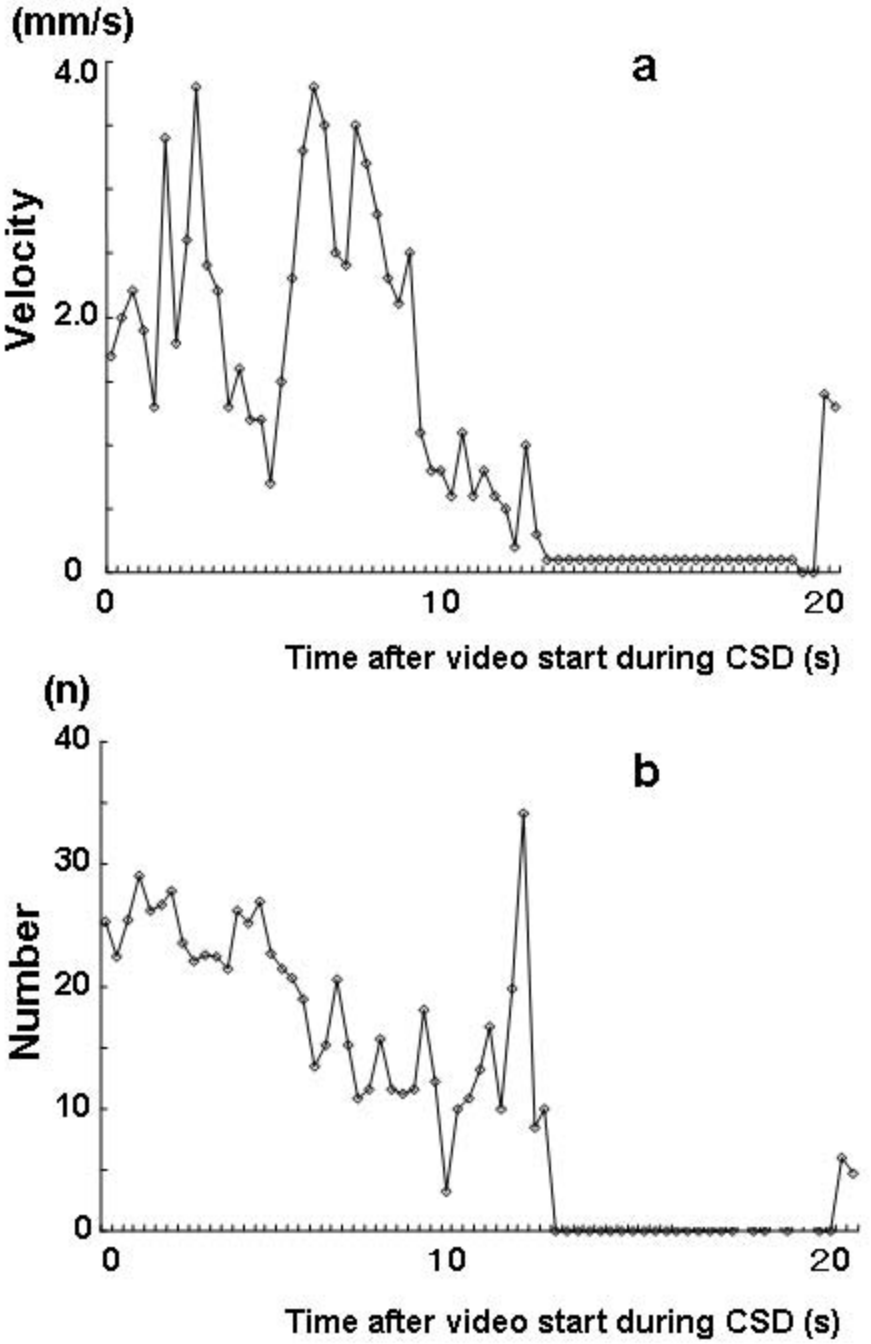
(mm/s)
a
4.0
2.0
0
Velocity
0
10
20
Time after video start during CSD (s)
(n)
b
40
30
20
10
0
Number
0
10
20
Time after video start during CSD (s)

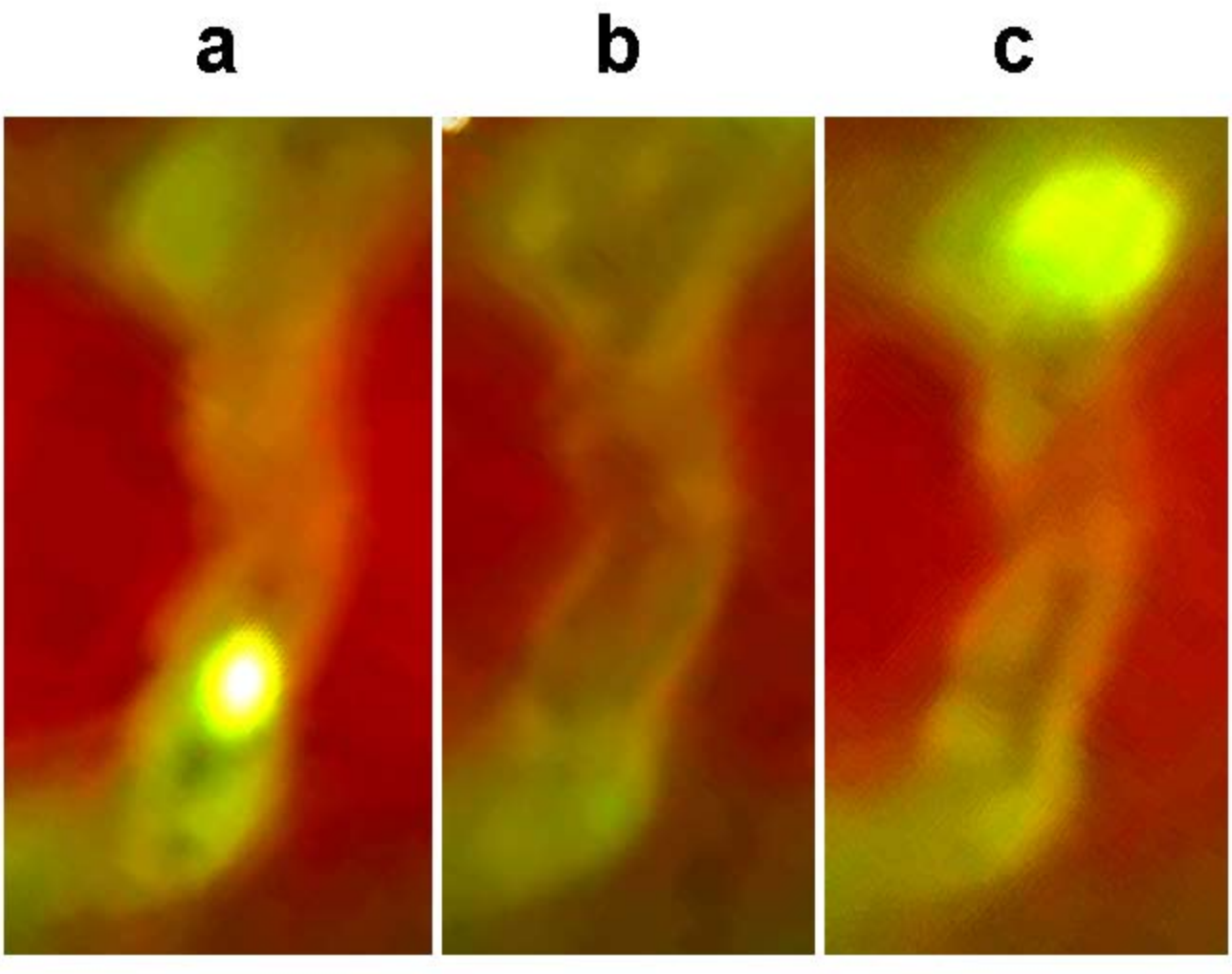
a
b
c

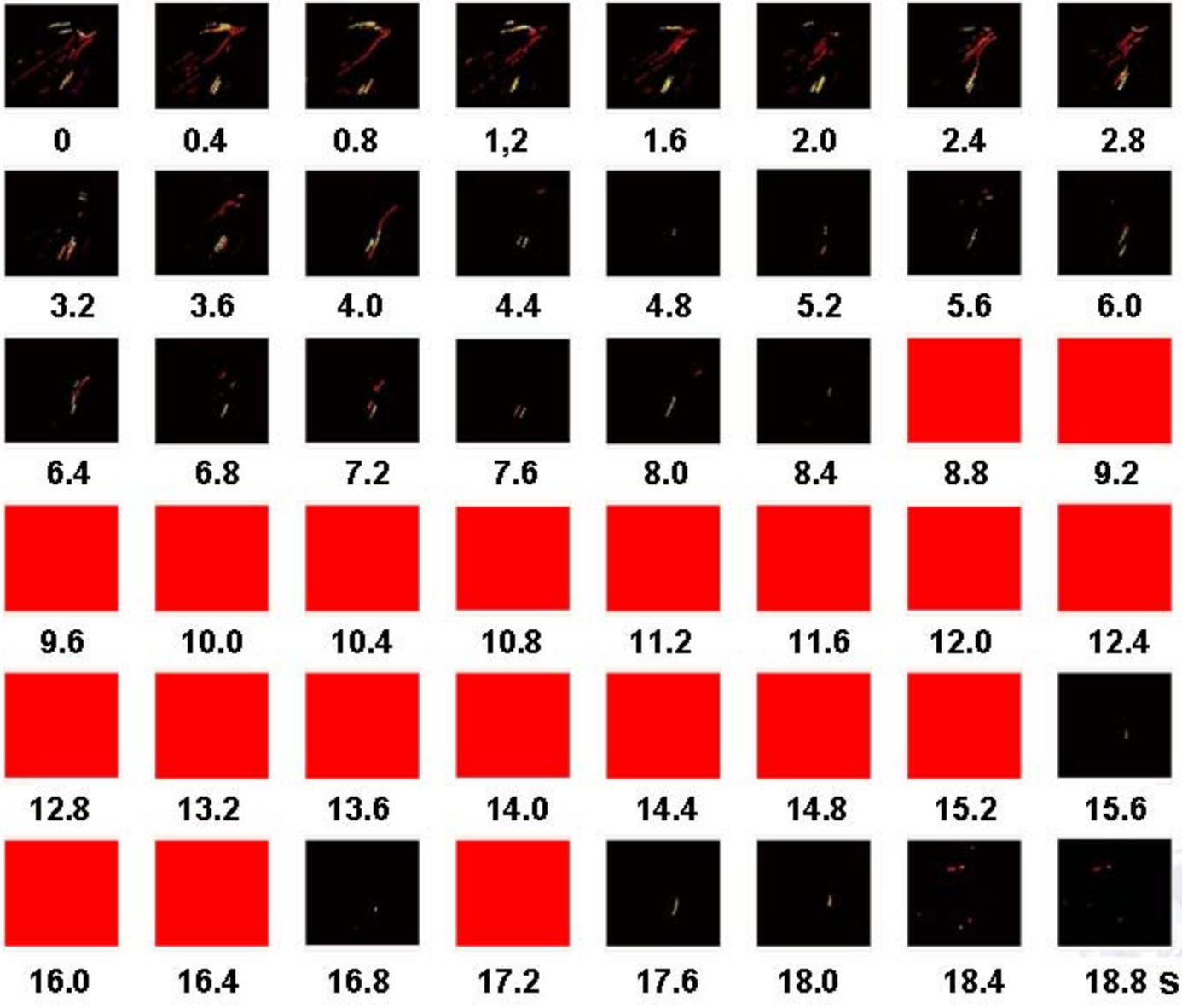
0
0.4
0.8
1,2
1.6
2.0
2.4
2.8
3.2
3.6
4.0
4.4
4.8
5.2
5.6
6.0
6.4
6.8
7.2
7.6
8.0
8.4
8.8
9.2
9.6
10.0
10.4
10.8
11.2
11.6
12.0
12.4
12.8
13.2
13.6
14.0
14.4
14.8
15.2
15.6
16.0
16.4
16.8
17.2
17.6
18.0
18.4
18.8 s

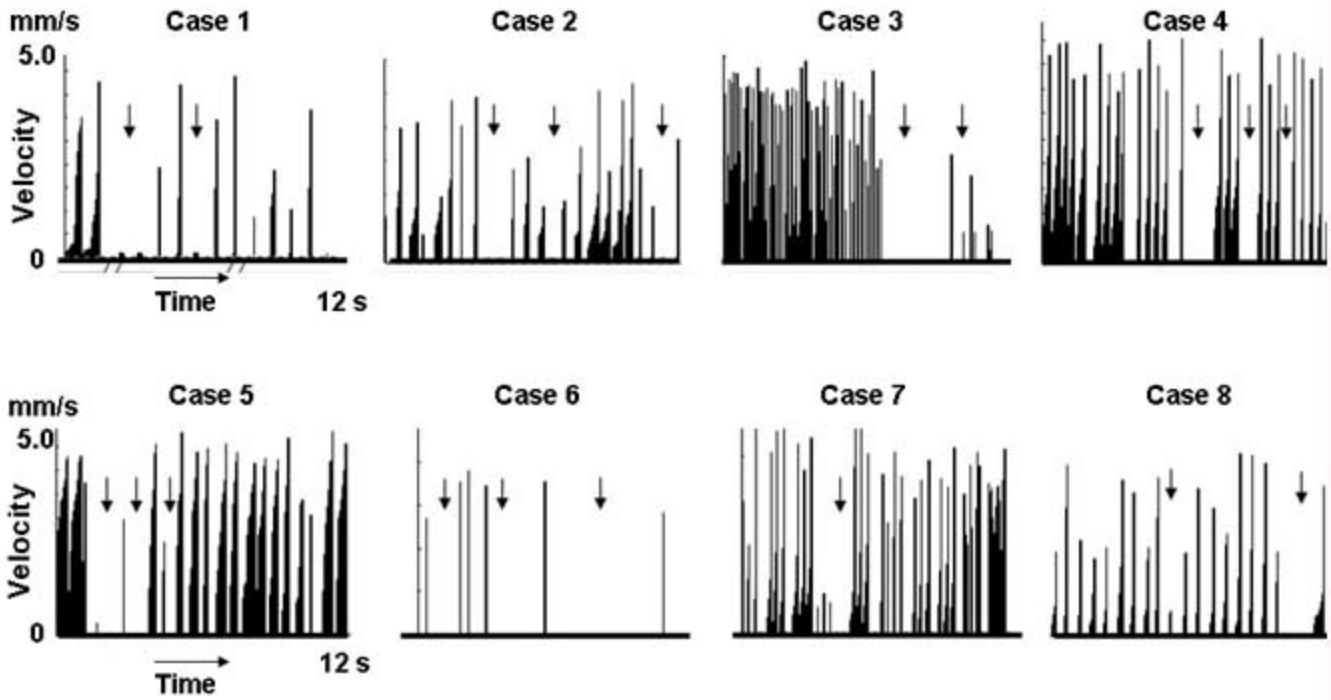
mm/s
Case 1
5.0
Velocity
0
Time
12 s
Case 2
Case 3
Case 4
mm/s
Case 5
5.0
Velocity
0
Time
12 s
Case 6
Case 7
Case 8